Incorporation of Am into the superconductor-related phase Pr_2CuO_4

S. Skanthakumar, C. W. Williams, and L. Soderholm
Chemistry Division, Argonne National Laboratory, Argonne, Illinois 60439, USA
(Received 24 September 2002; revised manuscript received 10 February 2003; published 22 August 2003)

$Pr_{1.85}Am_{.15}CuO_4$ has been synthesized and found to have a structure consistent with the T'-phase electron superconductors. X-ray diffraction, x-ray-absorption spectroscopy studies, and magnetic-susceptibility results are all used to conclude that Am is tetravalent in this Cu-oxide host. Despite the hole doping of the parent Pr_2CuO_4 compound by Am^{4+}, magnetic measurements show that the $Pr_{1.85}Am_{.15}CuO_4$ sample does not superconduct, despite the observation that a Ce-doped sample made under the same condition exhibits a diamagnetic signal at low temperatures and small applied fields. The absence of superconductivity in the Am-doped sample is discussed in terms of a magnetic model for the suppression of T_c. The presence of Am^{4+} in this sample precludes the formation of $Am_{1.85}Ce_{.15}CuO_4$, which has been predicted to superconduct.

DOI: 10.1103/PhysRevB.68.064510 PACS number(s): 74.72.−h, 74.10.+v, 61.10.Ht, 61.10.Nz

I. INTRODUCTION

$Am_{2-x}Ce_xCuO_4$ (Am, $Z=95$) has recently been predicted to superconduct with a T_c of 24 K.[1] It is argued that this phase should form a homolog of the T' structure[2–4] found for $R_{2-x}M_xCuO_4$ (R^{3+}=Pr-Eu, Cm; M^{4+}=Ce, Th) and that, once synthesized, it could be used to distinguish between charge-reservoir and cuprate-plane models for superconductivity.[1] More generally, it can be argued that if Am can be incorporated into the T' phase, the conductivity and magnetic properties of this material should provide valuable insights into the role of unpaired spin density in suppressing superconductivity. As has been previously proposed[5,6] a lighter lanthanide, such as Pr^{3+}, or an actinide with a nonsinglet ground state, such as Cm, may suppress superconductivity via a hybridization of radially extended, magnetic, f states with Cu-O bands. It is argued that this T_c suppression has its origin in enhanced magnetic interactions. This argument is supported by the anomalously high magnetic-ordering temperatures seen for a variety of Pr (Refs. 7–9) and Cm (Refs. 10–13) high-T_c analogs.

The chemistry of Am, including size and charge considerations, as well as the trivalent/tetravalent redox couple are very similar to those of Ce. Am has two stable oxidation states in solid samples, the trivalent state, as exemplified by Am_2O_3 and the tetravalent state, as exemplified by AmO_2.[14] Am^{3+} has an ^6f configuration, so assuming Russell-Saunders coupling it has a $J=0$, singlet ground state irrespective of the site symmetry, and therefore no local moment at low temperature.[15,16] This is to be compared with Cm^{3+} ($Z=96$), which has an ^7f configuration and therefore a spherically symmetric ground state, with a large local moment that is uninfluenced, to first order, by the crystalline-site symmetry.[12] Am^{4+} has an ^5f configuration and, according to simple coupling arguments, a $J=5/2$ ground state. The local moment on Am^{4+} can be expected to interact with surrounding ions because the $5f$ wave functions are more radially extended than their $4f$ counterparts.

$Am_{2-x}Ce_xCuO_4$ has been predicted to form and to be superconducting,[1] although chemical precident argues against the formation of this phase. Preliminary synthetic efforts in this laboratory to form Am_2CuO_4 have been unsuccessful, resulting instead in AmO_2 and reduced Cu. Neither the Ce nor Am phases of $RBa_2Cu_3O_7$ nor R_2CuO_4 have been reported to form. In addition, $Pb_2Sr_2AmCu_3O_8$ has been reported,[17] but Am is tetravalent in this superconductor-related phase. The objectives of the work reported herein are the synthesis and characterization of a T'-phase sample containing Am. $Pr_{2-x}Am_xCuO_4$ has been chosen for study for several reasons. The parent compound Pr_2CuO_4 has been well characterized.[8,18] Pr is trivalent, with an $^3H_4$ ground term that has a singlet ground state in the crystal field imparted by the lattice.[19] Doping with Ce^{4+} or Th^{4+},[2] both of which are diamagnetic, results in a superconducting phase. The R_2CuO_4 lattice is able to incorporate either trivalent or tetravalent ions at the 7% doping level of the R^{3+} site. The incorporation of Am^{3+}, with its singlet ground state, would provide direction for making a phase appropriate for studying predictions arising from either the charge-reservoir or magnetic suppression models. The incorporation of Am^{4+} would provide a direct opportunity to study the influence of a magnetic ion, with radially extended valence states, on superconducting properties.

II. EXPERIMENT

^{243}Am, atomic number 95, is a manmade, radioactive element (α decay, $t_{1/2}=7.37\times10^3$ yr). All experiments with this isotope are performed in specialized laboratories using procedures designed and approved to minimize radiological and chemical hazards. The limited availability, together with radiation exposure concerns, require the use of only mg quantities and thereby limit studies to small sample sizes.

A polycrystalline sample of $Pr_{1.85}Am_{0.15}CuO_4$ was prepared following similar solid-state reaction techniques, which were optimized for the production of high-purity, superconducting $Pr_{1.85}Ce_{0.15}CuO_4$.[4] Stoichiometric ratios of americium oxalate [$Am_2(C_2O_4)_3$], Pr_6O_{11}, and CuO were mixed and prefired at 900 °C in air. The sample was reground and sintered at 1100 °C in air. This procedure was repeated until the x-ray-diffraction data showed primarily a single phase. Finally the sample was resintered at 900 °C under an N_2 atmosphere for 15 h and rapidly cooled to room tempera-

ture. Similarly prepared $Pr_{1.85}Ce_{0.15}CuO_4$ samples were found to superconduct with a T_c of 20 K.

X-ray-diffraction data were obtained over the angular range 5° to 150° at room temperature from a Scintag theta-theta diffractometer using Cu K_a (1.5405 and 1.5443 Å) radiation. Approximately 5 mg of the sample, encapsulated under a Kapton film as a safety requirement, was used for the diffraction experiment. The data were analyzed using the general structure analysis system (GSAS) program.[20]

X-ray-absorption experiments were conducted on powder samples at room temperature on the BESSRC bending magnet beamline 12-BM-B at the Advanced Photon Source following safety protocols and procedures outlined by the Actinide Facility. The beamline is equipped with a Si (111) double-crystal monochromator and a Pt mirror that is required to remove higher-order harmonics that are present because of the high critical energy of the Advanced Photon Source ring. The Zr *K* edge was used to calibrate the monochromator energy at 17 998 eV. AmF_3 and $Pb_2Sr_2AmCu_3O_8$ (Ref. 17) were used as trivalent and tetravalent standards, respectively. Data were collected in transmission and fluorescence modes using a Canberra multielement Ge detector. The extended x-ray-absorption fine-structure (EXAFS) data analysis methodology is described elsewhere.[21] WINXAS data analysis software[22] was used to fit the EXAFS data. FEFF8.01 (Ref. 23) was used to obtain the phase and amplitude functions required for the EXAFS refinement.

The magnetic-susceptibility measurements were conducted on a Quantum Design superconducting quantum interference device, under an applied field of 500 G, over a temperature range of 5–320 K. In addition, magnetization data were collected at 5 K in the field range of 0–50 000 G. The 17.8-mg sample was doubly encapsulated in aluminum containers, which were run independently to determine the background correction to the data. The error on the measured susceptibility is large because the sample size is small, the sample itself has a very low susceptibility, and the encapsulation contributes a high background. The sample was checked for superconductivity under a remnant field.

III. RESULTS

A. Powder diffraction

X-ray powder diffraction is used to identify the structure formed and its phase purity. The powder pattern obtained from $Pr_{1.85}Am_{.15}CuO_4$ is shown in Fig. 1. The moderate data quality reflects the small amount of sample (5 mg total) necessitated by the use of ^{243}Am and the need for sample encapsulation. Nevertheless, the data have narrow, well-defined diffraction lines, indicating that the sample is well crystallized. The observed peaks can be indexed assuming two crystalline phases, one consistent with the tetragonal lattice previously reported for Pr_2CuO_4 (Ref. 24) and the other, a minor impurity phase, whose lines are consistent with Pr_6O_{11}.[25] There is no evidence indicating the presence of AmO_2, which would be the expected Am impurity phase. The absence of AmO_2 lines in the diffraction pattern shows that the Am must be incorporated into the Pr sample because

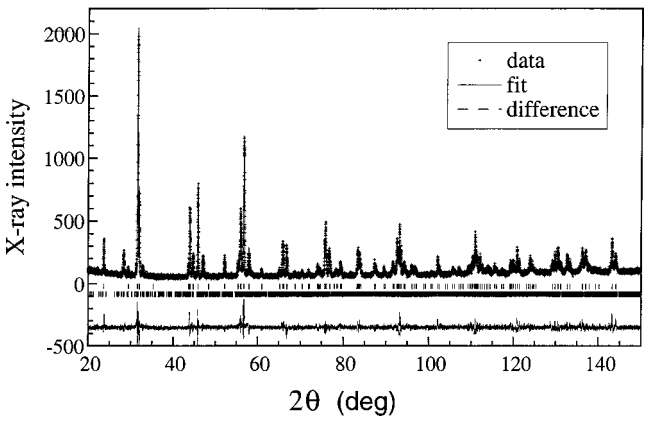

FIG. 1. Room-temperature x-ray-diffraction data obtained on a Scintag theta-theta diffractometer, operating with a copper source. The data are compared with their best fit over the angular range of 20° to 150° in 2θ. The fit includes 8.5-wt % Pr_6O_{11} as a second phase. The two sets of vertical lines indicate the positions of Bragg peaks originating from $Pr_{1.85}Am_{0.15}CuO_4$ (top) and Pr_6O_{11} (bottom).

Am is a strong x-ray scatterer and AmO_2 has the $Fm3m$ structure, which has most of its scattering intensity centered in very few diffraction lines.

The lattice constants, determined for the $Pr_{1.85}Am_{.15}CuO_4$ phase, are $a=3.9607(1)$ and $c=12.1676(2)$ Å. These lattice constants are compared with those from other R_2CuO_4-based compounds in Table I. The *a* axis of the parent compound Pr_2CuO_4 is comparable with that observed for the Am-doped sample, whereas the *c* axis is considerably shorter for the Am-doped compound. This shortening of the *c* axis with doping is also seen with Ce doping. Since trivalent Am is comparable in size with trivalent Pr, this result indicates that tetravalent Am is substituting for trivalent Pr. In addition, the c/a ratio for the Am-doped Pr_2CuO_4 sample is 3.072, which is slightly smaller than the value of 3.085 found for the parent compound. A similar contraction of the c/a ratio with doping was also observed for $Cm_{1.85}Th_{.15}CuO_4$.[11] A comparison of the c/a ratios of the R_2CuO_4-based samples in Table I reveals that the value obtained for $Pr_{1.85}Am_{.15}CuO_4$ is similar to all of the other entries in the table except for the La analog. All entries show doping with a tetravalent ion, except for the La analog, in which Ba^{2+} substitutes for La^{3+}. The c/a ratio can be used to determine whether a sample is isostructural with the hole-doped superconductors, as exemplified by the La/Ba analog, or the electron superconductors, as exemplified by the Pr/Ce analog. The Am-doped Pr sample follows the trend established for the electron superconductors.

The x-ray powder pattern shown in Fig. 1 was refined from a model based on the $Pr_{1.85}Ce_{.15}CuO_4$ structure. Using the space group $I4/mmm$ (No. 139) Pr and Am are disordered on the 4*e* site, 0 0 *z*, Cu is located at the 2*a* site, 0 0 0, one of the two crystallographically inequivalent oxygens sits on the 4*c* site, 0 0.5 0, and the other sits on the 4*d* site, 0 0.5 0.25. The only structural variable, in addition to the lattice constants themselves, is the Pr/Am site *z* coordinate, which refines to 0.3515(2). In order to fit the experimental data adequately, it is necessary to include a contribution from

TABLE I. Lattice constants of representative R_2CuO_4 compounds. All compounds crystallize in the tetragonal space group $I4/mmm$. There are two different structure types within the $I4/mmm$ space group that have been shown for superconductors. If there is an oxygen located on the Wyckoff position $4e$, the sample is a hole superconductor, and it is referred to being in the T phase. In contrast, if the Wyckoff position $4d$ is occupied, the sample is an electron superconductor, and is referred to as being in the T' phase (Ref. 2). Numbers in parentheses following the lattice constants refer to the error in the last digit.

	Phase	a (Å)	c (Å)	c/a	References
La_2CuO_4		3.8026[a]	13.1669	3.4626	47
$La_{1.85}Ba_{0.15}CuO_4$	T	3.7873(1)	13.2883(3)	3.5086	47
Pr_2CuO_4	T'	3.96016(4)	12.2189(1)	3.0855	this work
$Pr_{1.85}Ce_{0.15}CuO_4$	T'	3.9639(2)	12.1601(7)	3.0677	this work
Nd_2CuO_4	T'	3.9417(6)	12.163(6)	3.0857	48
$Nd_{1.85}Ce_{0.15}CuO_4$	T'	3.9450(6)	12.078(9)	3.0616	48
Cm_2CuO_4	T'	3.946(2)	12.181(5)	3.0869	11, 12
$Cm_{1.85}Th_{0.15}CuO_4$	T'	3.952(1)	12.13(1)	3.069	11
$Pr_{1.85}Am_{0.15}CuO_4$	T'	3.9607(1)	12.1676(2)	3.0721	this work

[a]Averaged from the orthorhombic room-temperature structure.

Pr_6O_{11}. This known structure is included as a second phase in the fit, with the cell constants and the scale factor as the only fitted parameters. The refined lattice constants are 6.687(13), 11.602, and 12.829(19) Å with a beta angle of 100.70(16)°. The refined scale factors show that there is about 8.5 wt % of the Pr_6O_{11} phase in the sample. The agreements of the refined structure with the experimental data are $R_{wp}=0.1209$, $R_p=0.0956$, and $\chi^2=1.592$. Although problems associated with such small sample sizes, together with the need for encapsulation, prohibit the acquisition of better data, the lattice constants determined by GSAS fitting unequivocally show that the sample crystallizes in the T' structure of Pr_2CuO_4.

Although powder x-ray-diffraction data from a heavy-metal, mixed oxide normally do not allow the accurate determination of metal-oxygen distances, the location of both oxygens on special positions with no variable parameters means that the Pr/Am-O distances are directly established from the lattice constants and the Pr/Am z coordinate, both of which are well determined by the refinement. Consequently, the results of the GSAS refinement of the powder x-ray data are used to reliably determine the Pr/Am-O bond distances in $Pr_{1.85}Am_{0.15}CuO_4$, which are 2.3355(4) and 2.6787(4) Å.

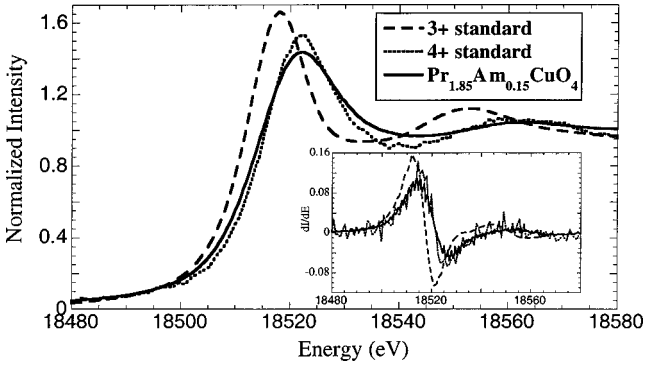

FIG. 2. Am L_3-edge XANES data from $Pr_{1.85}Am_{0.15}CuO_4$ are compared with a trivalent (AmF_3) and tetravalent ($Pb_2Sr_2AmCu_3O_8$) standard. The first derivatives of the edge spectra are shown in an inset. The 3-eV shift to higher energy of the Am^{4+} edge energy over that obtained from Am^{3+} is consistent with other studies that show similar shifts between trivalent and tetravalent actinide samples (Ref. 26).

B. XANES

Am L_3-edge x-ray-absorption near-edge structure (XANES) data are used to determine the valence state of Am in $Pr_{1.85}Am_{0.15}CuO_4$. The XANES spectrum obtained from Am in $Pr_{1.85}Am_{0.15}CuO_4$, together with those from trivalent (AmF_3) and tetravalent Am standards [$Pb_2Sr_2AmCu_3O_8$ (Ref. 17)] are shown in Fig. 2. The first derivatives of the normalized intensities, used to determine the edge positions, are shown in the inset. As seen from the data analysis in Table II, the fingerprint of a trivalent Am spectrum is an absorption energy (first peak in the derivative spectrum) at 18 512 eV, whereas the first derivative of the tetravalent Am absorption energy is 18 515 eV. The observed shift in edge energy of 3 eV between trivalent and tetravalent Am is consistent with the 3–4-eV difference in edge energy that is seen for other trivalent/tetravalent actinide edges.[26] A comparison of the L_3-edge energy of our sample with those of the stan-

TABLE II. A comparison of the fits of L_3 XANES data from $Pr_{1.85}Am_{0.15}CuO_4$ with trivalent (AmF_3) and tetravalent ($Pb_2Sr_2AmCu_3O_8$) (Ref. 17) Am standards. Data were detected in the transmission (T) or fluorescence (F) mode. The edge energies are calibrated by setting the first derivative of the Zr K edge to 17 998 eV. Errors in the energies are ±1 eV.

	Detection mode	Peak maximum	First derivative maximum
AmF_3	T	18 518	18 512
$Pb_2Sr_2AmCu_3O_8$	F	18 522	18 515
$Pr_{1.85}Am_{0.15}CuO_4$	F	18 522	18 515

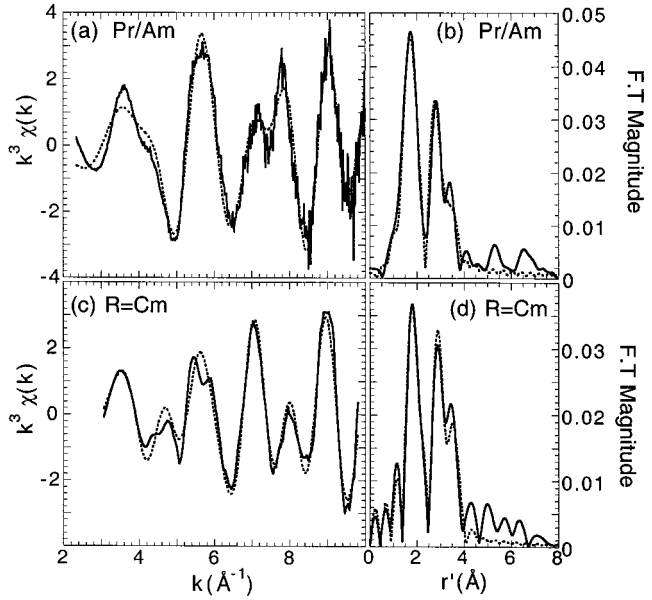

FIG. 3. $k_3\chi(k)$ EXAFS (left panel) and Fourier-transform (right panel) data without phase-shift correction for [(a) and (b)] americium L_3-edge data from $Pr_{1.85}Am_{0.15}CuO_4$ and [(c) and (d)] curium L_3-edge data from Cm_2CuO_4. The data are shown as solid lines and the fits as dashed lines. Similarity in the data from Am and Cm is used to argue that Am sits on the Pr site in the doped sample.

dards clearly demonstrates that Am is tetravalent in $Pr_{1.85}Am_{0.15}CuO_4$, a finding in support of the diffraction results.

C. EXAFS

Am L_3 EXAFS spectroscopy is used to determine the coordination environment about Am in $Pr_{1.85}Am_{0.15}CuO_4$. The EXAFS data, together with their Fourier transform (FT), are compared with similar data from Cm_2CuO_4 in Fig. 3. Cm_2CuO_4 has previously been shown to be isostructural with Pr_2CuO_4.[12] A comparison of the two FT's reveals the similarity in coordination environments of the two f ions, thus confirming that Am substitutes at the Pr lattice position. A fitting of the Am EXAFS data results in metrical parameters listed in Table III. The Am coordination environment consists of four oxygens at 2.19(2) Å and four oxygens at 2.62(3) Å. These distances are statistically different from the values of 2.3366(4) and 2.6787(4) Å determined from the diffraction data. The significantly shorter Am-O bond distances determined from EXAFS data reflect the local lattice contraction that is expected because Am^{4+} is a smaller, more highly charged ion than the Pr^{3+}, for which it is substituting. EXAFS spectroscopy is a single-ion probe that measures the Am coordination directly whereas the diffraction data measures the average coordination environment about the Pr/Am site, which will be dominated by the Pr-O distance. A similar comparison can be made for Cm coordination in Cm_2CuO_4, as determined by Cm L_3 EXAFS data. Trivalent Cm has near-neighbor oxygen distances, as determined by EXAFS data, of 2.30(2) and 2.63(3) Å. The shorter distances observed by EXAFS spectroscopy for Am-O over Cm^{3+} again reflect the difference in oxidation state between the two ions. Trivalent Am has a larger ionic radius than does trivalent Cm. Therefore the shorter Am-O distance compared to the Cm-O distance supports the XANES result that it is tetravalent Am that substitutes for Pr^{3+} in the Pr_2CuO_4 lattice.

The average Am-O distance of 2.40 Å in $Pr_{1.85}Am_{0.15}CuO_4$ is longer than the Am^{4+}-O_8 distance of 2.327 Å in AmO_2 (Ref. 27) and 2.22 Å obtained for $Pb_2Sr_2AmCu_3O_8$ (Ref. 17) but smaller than the distance of 2.53 Å estimated from the lattice constants of $AmScO_3$,[28] in which Am is trivalent. It should be noted that the Am coordination in $Pr_{1.85}Am_{0.15}CuO_4$ is rather distorted, with a 14% difference in oxygen bond lengths for the nearest-neighbor coordination sphere.

IV. MAGNETIC SUSCEPTIBILITY

The magnetic responses of $Pr_{1.85}Am_{0.15}CuO_4$ and $Pr_{1.85}Ce_{0.15}CuO_4$, as a function of applied field at low temperature, are compared in Fig. 4. The two samples are the same size, and were prepared and measured using the same conditions. The behavior of the Ce-doped analog demonstrates the expected superconductivity in this phase. By contrast, the Am analog shows no evidence of superconductivity. The occurrence of superconductivity in copper oxides is known to be very sensitive to preparative conditions, particularly oxygen stoichiometry and annealing procedures. The preparative conditions for the synthesis of $Pr_{1.85}Am_{0.15}CuO_4$ were based on the optimized procedure for a single phase, superconducting $Pr_{1.85}Ce_{0.15}CuO_4$ sample, which is seen to be superconducting. The effects of radiation damage are un-

TABLE III. Results of the fits of $k^3\chi(k)$ Am and Cm L_3-edge EXAFS data from $Pr_{1.85}Am_{0.15}CuO_4$ and Cm_2CuO_4 (Ref. 12). Estimated uncertainties are 1% for all distances. Coordination numbers are fixed based on crystal structure. S_0^2 has been fixed at 1 for all fits (Ref. 26). Values of N are fixed and E^0 is fixed to the O 1 value.

	$R=$Am				$R=$Cm			
	N	r (Å)	σ^2 (Å)	E_O (eV)	N	r (Å)	σ^2 (Å)	E_O (eV)
O 1	4	2.19	0.0086	0.993	4	2.30	0.0072	6.017
O 2	4	2.62	0.016	c	4	2.63	0.0117	c
Cu	4	3.31	0.0095	c	4	3.31	0.0099	c
R	4	3.57	0.014	c	4	3.58	0.0144	c

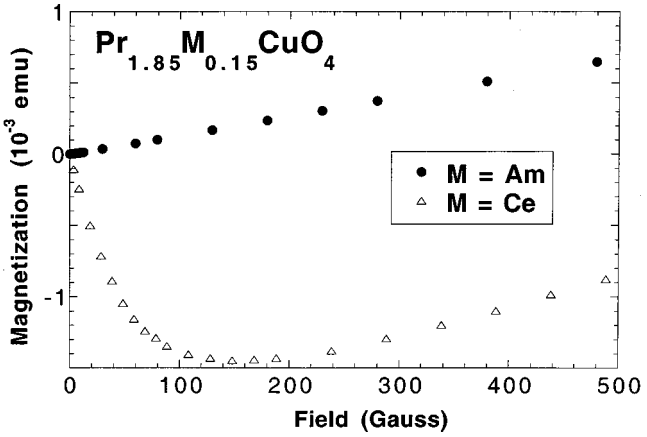

FIG. 4. Magnetization vs field data obtained from polycrystalline samples of $Pr_{1.85}Ce_{0.15}CuO_4$ and $Pr_{1.85}Am_{0.15}CuO_4$. The data, which were obtained at a temperature of 5 K, are shown after correction for the container contribution. The diamagnetic signal at low fields shows that the $Pr_{1.85}Ce_{0.15}CuO_4$ sample is superconducting. In contrast, there is no evidence for superconductivity in $Pr_{1.85}Am_{0.15}CuO_4$.

likely as the source of T_c suppression because ^{243}Am ($t_{1/2}$ = 7340 yr; α decay) was used in the preparation, which has a relatively long half life, and because the samples were measured within 6 days of preparation. Characterization of the structure, coordination environment, and dopant oxidation state is consistent with that expected for a superconducting sample.

The magnetic susceptibility of $Pr_{1.85}Am_{0.15}CuO_4$, obtained as a function of temperature, is shown in Fig. 5. These data are analyzed assuming Curie-Weiss behavior, $\chi = C/(T+\theta) + \chi_{TIP}$, where C and θ are Curie and Weiss constants and χ_{TIP} is the temperature-independent contribution to the susceptibility. C is related to the effective magnetic moment $\mu_{eff} = (3kC/N_0\beta^2)^{1/2}$ in which N_0 is Avogadro's number and β

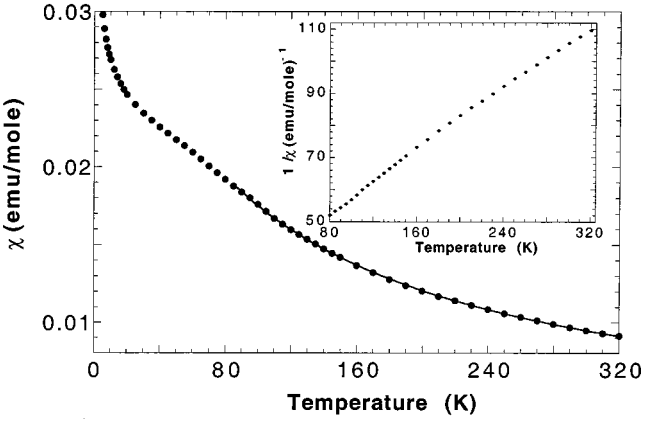

FIG. 5. The magnetic susceptibility, obtained as a function of temperature ($5 < T < 320$ K), for $Pr_{1.85}Am_{0.15}CuO_4$. The data, which were obtained under an applied field of 500 G, are shown after correction for the container contribution. There is no evidence of superconductivity down to the lowest temperature measured. The solid line represents the fit to the data over the temperature range 80–320 K. The inset show the same data as a Curie-Weiss plot.

is the bohr magneton (0.927×10^{-20} erg/Oe). The effective moment determined from a fit to data in Fig. 5, over the temperature range $85 < T < 320$ K, is $4.7(2)\mu_B$/f.u., and measured χ_{TIP} and θ are 0.0022 emu/mol f.u. and 81 K, respectively. The measured effective moment compares with the free-ion value for $Pr_{1.85}Am_{0.15}CuO_4$ of $4.88\mu_B$, calculated assuming pure Russell-Saunders free-ion moments for Pr^+ of $3.58\mu_B$ and for Am^{4+} of $0.845\mu_B$. A more appropriate comparison includes an effective moment for Pr of $3.53\mu_B$, which has been determined from a full crystal-field analysis of inelastic-neutron-scattering data.[8,19] The Pr contribution is determined using the wave functions and energy levels determined from the inelastic neutron scattering fitting to calculate susceptibilities as a function of temperature. This susceptibility data is then fitted to the Curie-Weiss law in the same manner used to fit the experimental data. This procedure results in a calculated moment over this temperature range of $4.81\mu_B$, little changed from the free-ion case. The Cu moment was not included in the calculation because Cu spins in Pr_2CuO_4 have been shown to order antiferromagnetically at about 255 K (Ref. 18) and to exhibit strong two-dimensional antiferromagnetic correlations even at temperatures as high as $2T_N$.[29] Strong Cu moment correlations that persist above T_N obscure evidence for the transition in the susceptibility data. Furthermore, it has also been demonstrated that the observed susceptibility of Pr_2CuO_4 is adequately described with contributions only from the Pr sublattice over the temperature range of interest.[19,30]

Whereas the susceptibility from $Pr_{1.85}Am_{0.15}CuO_4$, measured at higher temperatures, compares well with single-crystal data from the parent compound,[30] it differs markedly at lower temperatures. The parent compound has a temperature-independent susceptibility at temperatures below about 50 K that is not observed in the Am-doped material. In addition to confirming that the Cu spins are ordered in the parent compound at this temperature, the observed temperature-independent paramagnetism also confirms the neutron-scattering assignment of an isolated Γ_3 singlet ground state for Pr^{3+}, with a magnetic Γ_5 at 18 meV.[19] The incorporation of Am^{4+} into the parent structure influences the low-temperature susceptibility, which has a considerable temperature dependence below 50 K. The magnitude of the measured susceptibility (an estimated effective moment of about $1.2\mu_B$ over the temperature range 10–50 K) is significantly more than expected simply from the addition of 7-mol % Am^{4+}. The observed enhancement of the low-temperature susceptibility for the doped sample may be the result of a change in the copper ordering, it may result from a change in the crystal field experienced at the Pr^{3+} site, or it may indicate hybridization of the localized Am f states with the Cu-O band states. Similar behavior has been previously observed for $PrBa_2Cu_3O_7$ (Ref. 31) and $Pb_2Sr_2PrCu_3O_8$ (Ref. 5) samples that have been doped with Ca.

V. DISCUSSION

$Pr_{1.85}Am_{0.15}CuO_4$ forms and has a structure consistent with the T'-phase electron superconductors. Although trivalent Am, as the oxalate, was used in the synthesis, and the

parent compound can accommodate either the trivalent or tetravalent Pr substitutions, Am is tetravalent in the final product. The determining factor for the Am oxidation state is its reduction potential relative to the chemical potential of the Pr_2CuO_4 lattice, which is determined primarily by Cu^{2+}. Contrary to previous prediction,[1] Am^{3+} effectively reduces Cu^{2+}. This finding is consistent with our experimental attempts to make the pure Am_2CuO_4 phase, all of which produced oxidized $Am^{4+}O_2$ and reduced Cu, with no evidence of the target phase. The inability to make the Am analog of Pr_2CuO_4 is also consistent with previous attempts to make Ce_2CuO_4. The pure Ce compound does not form because the Ce reduction potential is sufficiently large relative to that of Cu, that is, Ce is oxidized and Cu is reduced. In general, the Ce and Am analogs of the superconductor-related Cu oxides do not form unless the lattice can incorporate a tetravalent ion. Specifically, the $RBa_2Cu_3O_7$ series does not accept a tetravalent ion and therefore does not form the Ce (Ref. 32) or Am (Ref. 33) analog. In contrast, $Pb_2Sr_2RCu_3O_8$ does incorporate tetravalent ions and both the Ce^{4+} (Ref. 34) and Am^{4+} (Ref. 17) analogs have been synthesized and characterized. Although Ca doping results in single phases for both these compounds, neither is superconducting.

In the case under study here, the ease with which Am^{3+} is oxidized is intermediate between Pr^{3+} (which is harder to oxidize) and Ce^{3+} (which is easier to oxidize). For the series of complex copper oxides that have been studied to date, it appears that Am and Ce are tetravalent in all cases, whereas Pr and Tb are trivalent. This example can be compared with the perovskite series $BaRO_3$, which provides more of an oxidizing environment for the *R* ion. This ternary Ba-oxide series, with the gadolium orthoferrite structure, includes R^{4+} analogs that are stabilized for $R=$Ce,[35] Pr,[35,36] and Tb,[35,37] as well as Th,[38] U,[39] Np,[40] Pu,[41] Am,[42] Cm,[43,44] and Cf.[45] Although there was a previous report of the stabilization of Dy^{4+}, it was independently determined that Dy is trivalent, and substitutes into the lattice with oxygen defects.[46]

$Pr_{1.85}Am_{0.15}CuO_4$ is not superconducting. Am^{4+} substitutes into the R_2CuO_4 structure in the same manner as does Ce^{4+} or Th^{4+}. Based on simple structural and charge-transfer arguments, $Pr_{1.85}Am_{0.15}CuO_4$ should exhibit very similar electronic behavior to the Ce and Th analogs. As demonstrated in Fig. 4, the Pr-Ce analog, prepared under identical conditions, superconducts at low temperatures. We argue that the anomalous behavior of the Am-doped material results from the local moment of Am^{4+}. The unpaired spins reside of $5f$ orbitals, which are expected to be more radially extended than their $4f$ counterparts that form superconducting phases. The presence of a magnetic moment in these extended orbitals is argued to suppress the superconductivity through hybridization.[6] It is this hypothesis that drove the initial interest in studying Am_2CuO_4 and its electron-doped analog. Whereas Am^{3+} has no magnetic moment, Am is incorporated into Pr_2CuO_4 as the tetravalent ion, which does carry a local moment.

The absence of superconductivity in this sample is consistent with the behavior of Cm_2CuO_4 and other nonsuperconducting samples that carry a local moment, in radially extended orbitals, on the *R* site. In addition to suppressing superconductivity, there is also a notable change in the low-temperature magnetic properties upon doping. Whereas the parent compound exhibits only a temperature-independent susceptibility below 50 K, the Am-doped sample has a marked temperature dependence on its measured susceptibility over this temperature range.

It should be noted that superconductivity in a sample containing an *f* ion with radially extended *f* orbitals, but with no unpaired spins, remains to be demonstrated. Such a sample would provide insight into the relative roles of hybridization and localized moments in the suppression of high-temperature superconductivity.

ACKNOWLEDGMENTS

This work has benefited from use of the BESSRC CAT at the Advanced Photon Source and the Actinide Facility, at the Argonne National Laboratory. This work is supported by the U.S. DOE, Basic Energy Sciences, Chemical Sciences, under Contract No. W-31-109-ENG-38.

[1] H. A. Blackstead and J. Dow, Phys. Rev. B **59**, 14 593 (1999).
[2] H. Takagi, S. Uchida, and Y. Tokura, Phys. Rev. Lett. **62**, 1197 (1989).
[3] M. B. Maple, MRS Bull. **15**, 60 (1990).
[4] Y. Tolura, H. Takagi, and S. Uchida, Nature (London) **337**, 345 (1989).
[5] U. Staub, L. Soderholm, S. Skanthakumar, R. Osborn, and F. Fauth, Europhys. Lett. **39**, 663 (1997).
[6] L. Soderholm and U. Staub, in *Electron Correlations and Magnetic Properties*, edited by A. Gonis, N. Kioussis, and M. Ciftan (Kluwer Academic, New York, 1999), pp. 115–136.
[7] W.-H. Li, J. W. Lynn, S. Skanthakumar, T. W. Clinton, A. Kebede, C.-S. Jee, J. E. Crow, and T. Mihalisin, Phys. Rev. B **40**, 5300 (1989).
[8] U. Staub and L. Soderholm, in *Handbook on the Physics and Chemistry of Rare Earths*, edited by J. K. A. Gschneidner, L. Eyring, and M. B. Maple (Elsevier Science, New York, 2000), Vol. 30, pp. 491–545.
[9] J. W. Lynn and S. Skanthakumar, in *Handbook on the Physics and Chemistry of Rare Earths*, edited by J. K. A. Gschneidner, L. Eyring, and M. B. Maple (Elsevier Science, New York 2001), Vol. 31, pp. 315–350.
[10] L. Soderholm, G. L. Goodman, U. Welp, C. W. Williams, and J. Bolender, Physica C **161**, 252 (1989).
[11] L. Soderholm, C. W. Williams, and U. Welp, Physica C **179**, 440 (1991).
[12] L. Soderholm, S. Skanthakumar, and C. W. Williams, Phys. Rev. B **60**, 4302 (1999).
[13] S. Skanthakumar, C. W. Williams, and L. Soderholm, Phys. Rev. B **64**, 144521 (2001).
[14] W. W. Schulz and R. A. Penneman, in *The Chemistry of the Actinide Elements*, edited by J. J. Katz, G. T. Seaborg, and L. R.

Morss (Chapman and Hall, London, 1986), Vol. 2, pp. 887–960.
[15] L. Soderholm, N. Edelstein, L. R. Morss, and G. V. Shalimoff, J. Magn. Magn. Mater. **54–57**, 597 (1986).
[16] L. Soderholm, J. Less-Common Met. **133**, 77 (1987).
[17] L. Soderholm, C. Williams, S. Skanthakumar, M. R. Antonio, and S. Conradson, Z. Phys. B: Condens. Matter **101**, 539 (1996).
[18] M. Matsuda, K. Yamada, K. Kakurai, H. Kadowaki, T. R. Thurston, Y. Endoh, Y. Hidaka, R. J. Birgeneau, M. A. Kastner, P. M. Gehring, A. H. Moudden, and G. Shirane, Phys. Rev. B **42**, 10 098 (1990).
[19] C.-K. Loong and L. Soderholm, Phys. Rev. B **48**, 14 001 (1993).
[20] A. C. Larson and R. B. V. Dreele, computer code GSAS (Los Alamos National Laboratory, Los Alamos, NM, 1990).
[21] B. K. Teo, *EXAFS: Basic Principles and Data Analysis* (Springer, Berlin, 1995).
[22] T. Ressler, J. Synchrotron Radiat. **5**, 118 (1998).
[23] J. J. Rehr, J. M. d. Leon, S. I. Zabinsky, and R. C. Albers, J. Am. Chem. Soc. **113**, 5135 (1991).
[24] D. E. Cox, A. I. Goldman, M. A. Subramanian, J. Gopalakrishnan, and A. W. Sleight, Phys. Rev. B **40**, 6998 (1989).
[25] J. Zhang, R. B. v. Dreele, and L. Eyring, J. Solid State Chem. **122**, 53 (1996).
[26] M. R. Antonio, L. Soderholm, C. W. Williams, J.-P. Blaudeau, and B. E. Bursten, Radiochim. Acta **89**, 17 (2001).
[27] T. D. Chikalla and L. Eyring, J. Inorg. Nucl. Chem. **30**, 133 (1968).
[28] C. Keller, U. Berndt, M. Debbabi, and H. Engerer, J. Nucl. Mater. **42**, 23 (1972).
[29] S. B. Oseroff, D. Rao, F. Wright, D. C. Vier, S. Schultz, J. D. Thompson, Z. Fisk, S. W. Cheong, M. F. Hundley, and M. Tovar, Phys. Rev. B **41**, 1934 (1990).
[30] C. K. Loong and L. Soderholm, in *Physical and Material Properties of High-Temperature Superconductors*, edited by S. K. Malik and S. S. Shah (Nova Science, New York, 1994), p. 257.
[31] U. Staub, L. Soderholm, S. R. Wasserman, A. G. O. Conner, M. J. Kramer, B. D. Patterson, M. Shi, and M. Knapp, Phys. Rev. B **61**, 1548 (2000).
[32] C. R. Fincher and G. B. Blanchet, Phys. Rev. Lett. **67**, 2902 (1991).
[33] L. Soderholm, C. W. Williams, and S. Skanthakumar (unpublished).
[34] S. Skanthakumar and L. Soderholm, Phys. Rev. B **53**, 920 (1996).
[35] A. J. Jacobson, B. C. Tofield, and B. E. F. Fender, Acta Crystallogr., Sect. B: Struct. Sci. **B28**, 956 (1972).
[36] M. Bickel, G. L. Goodman, L. Soderholm, and B. Kanellokopulos, J. Solid State Chem. **76**, 178 (1988).
[37] K. Tezuka, H. Yukio, Y. Shimojo, and Y. Morii, J. Phys.: Condens. Matter **10**, 11703 (1998).
[38] R. Scholder, D. Rade, and H. Schwarz, Z. Anorg. Allg. Chem. **362**, 149 (1968).
[39] Y. Hinatsu, J. Alloys Compd. **193**, 113 (1993).
[40] B. Kanellakopulos, C. Keller, R. Klenze, and A. H. Stollenwerk, Physica B **102**, 221 (1980).
[41] G. G. Christoph, A. C. Larson, P. G. Eller, J. D. Purson, J. D. Zahrt, R. A. Penneman, and G. H. Rinehart, Acta Crystallogr., Sect. B: Struct. Sci. **B44**, 575 (1988).
[42] C. Keller, in *Lanthanide/Actinide Chemistry*, edited by R. F. Gould (American Chemical Society, Washington, DC, 1967), p. 228.
[43] S. E. Nave, R. G. Haire, and P. G. Huray, Phys. Rev. B **28**, 2317 (1983).
[44] L. Soderholm, N. Edelstein, L. R. Morss, and G. Shalimoff, J. Magn. Magn. Mater. **54–57**, 597 (1986).
[45] J. R. Moore, S. E. Nave, R. G. Haire, and P. G. Huray, J. Less-Common Met. **121**, 187 (1986).
[46] L. Soderholm, L. R. Morss, and M. F. Mohar, J. Less-Common Met. **127**, 131 (1987).
[47] J. D. Jorgensen, H. B. Schuttler, D. G. Hinks, D. W. Capone, K. Zhang, and M. B. Brodsky, Phys. Rev. Lett. **58**, 1024 (1987).
[48] T. Uzumaki, N. Kamehara, and K. Niwa, Jpn. J. Appl. Phys., Part 2 **30**, L981 (1991).